Case Studies in Thermal Engineering 26 (2021) 101117

Contents lists available at ScienceDirect

Case Studies in Thermal Engineering

journal homepage: www.elsevier.com/locate/csite

Experimental study on heat transfer characteristics of closed thermosyphon at different volumes and inclination angles for variable vacuum pressures

Halit Arat [a,*], Oguz Arslan [b], Umran Ercetin [a], Abdullah Akbulut [a]

[a] Mechanical Engineering Department Kutahya Dumlupinar University Engineering Faculty, 43270, Kutahya, Turkey
[b] Mechanical Engineering Department Bilecik Seyh Edebali University Engineering Faculty, 11230, Bilecik, Turkey

ARTICLE INFO

Keywords:
Vacuumed pipe
Experimental analysis
Thermal performance
Variable saturation temperatures
Two-phase flow
Inclination angles

ABSTRACT

In this study, the thermal performance of vacuumed copper pipe has been experimentally investigated by using different volume values of 5 ml, 10 ml, 15 ml, and 20 ml with inclination angles of 45°, 60°, and 90° for variable vacuum pressures. For this purpose, the inner, outer diameter, and length of the vacuumed pipes filled with the distilled water were 26 mm, 28 mm, and 1500 mm, respectively. This copper pipe was vacuumed until the absolute pressure of 6.32 kPa and immersed in a heat source at a constant temperature of 82°C at the beginning of the experiments. The surface temperatures of the vacuumed pipes were measured at twenty different points by using K-type thermocouples in two different data loggers. All calculations were performed as variable saturation temperatures at variable vacuum pressures with changing the time. According to the results, the experimental boiling heat transfer coefficients showed a good agreement with the correlations in the literature. Also, the best thermal resistance was obtained in the vacuumed copper pipe with a water volume of 10 ml at the inclination angle of 90° until the end of the experiment.

1. Introduction

Day by day, people use more and more energy because of the advances in technology and comfortable life. Therefore, all countries should utilize their limited energy efficiently to meet this considerable energy demand [1]. For this purpose, the systems like the vacuumed pipes providing efficient heat transfer with phase transition between interfaces have started widely use nowadays [2]. Some of them have been used with nanofluids [3], while some are related to different types of heat pipes [4].

The vacuumed pipes provide efficient heat transfer with phase transition between interfaces due to the evaporating has started in low temperatures at vacuum conditions. The vacuumed pipe consists of three main parts: boiling, evaporating, and condensing sections [5]. When the fluid inside the vacuumed pipe is heated, it boils and evaporates, ascending to the top of the vacuumed pipe at a constant temperature. At this point, the rising steam begins to condensate, and two-phase flow occurs inside the heat pipe [6]. According to the literature, the mechanism playing a primary role in the two-phase flow is one of the most economical and practical methods [7,8]. Moreover, this mechanism has been used in different applications like flat-plate solar collector [9], absorption

* Corresponding author.
E-mail addresses: halit.arat@dpu.edu.tr (H. Arat), oguz.arslan@bilecik.edu.tr (O. Arslan), umran.ercetin@dpu.edu.tr (U. Ercetin), abdullah.akbulut@dpu.edu.tr (A. Akbulut).

https://doi.org/10.1016/j.csite.2021.101117
Received 1 May 2021; Received in revised form 25 May 2021; Accepted 27 May 2021
Available online 1 June 2021

refrigeration [10], flow boiling in microchannel [11], the pulsating heat pipe [12], etc. In this way, energy could be utilized more efficiently.

Jouhara et al. [13] have experimentally investigated the use of the water and ethanol-water azeotrope as working fluid in a two-phase closed thermosyphon with an inclined condenser section. Their thermosyphon was manufactured from a 22 mm outer diameter, 1.5 m long smooth copper tube with a tube wall thickness of 0.9 mm. Their study showed that the effective overall thermal resistance of the heat pipe was found to decrease with increasing power throughputs up to a value after which R was found to stabilize. Also, they reported that there was not a remarkable effect of the inclination angle (between 15° and 90°).

Sarafraz et al. [14] have experimentally studied a thermosyphon heat pipe's thermal performance and efficiency using biologically ecofriendly Ag/water nanofluids as working fluid. They fabricated the thermosyphon from the smooth copper tube with an inner diameter, outer diameters, and total length of 10.7 mm, 12 mm, and 280 mm, respectively. According to the results, the best thermal performance of thermosyphon was obtained at the filling ratio of 0.65 and inclination angle of 55° with wt.% = 0.4 of Ag/water nanofluids.

Gedik [15] has experimentally investigated the thermal performance of a two-phase closed thermosyphon considering different operating conditions like heating power inputs (200 W, 400 W, and 600 W), inclination angles (30°, 60°, and 90°), cooling water flow rates (10 L/h, 20 L/h, and 30 L/h), and working fluids (water, ethanol, and ethylene glycol). A copper thermosyphon that was 100 cm long had an inner and outer diameter of 18 mm and 19 mm, respectively, was used in the experiments. The results of this study showed that the water attained the highest heat transport capability among three working fluids for the operating heat input of 200 W and the cooling water flow rate of 10 L/h. Also, the heat transfer rate increased as the inclination angle increased, and water was more effective in terms of thermal performance at low cooling flow rates. At the same time, ethylene glycol was a more effective working fluid at higher flow rates.

Seo and Lee [16] have experimentally studied the thermal-hydraulic characteristics of an extended heat pipe with various length scales in a small number of studies in the literature. For this purpose, they have utilized the heat pipes manufactured using stainless pipe and had an inner diameter of 16.57 mm and lengths of 1 m, 2 m, and 3 m. According to their results, the entrainment limit points were affected by the L/D value of the heat pipe; the effect of L/D was formulated from experimental results.

Naresh et al. [17] have experimentally investigated the heat transfer from a wickless finned heat pipe charged with different self-rewetting fluids (hexanol, butanol, pentanol, heptanol). A copper pipe with a length of 500 mm, an outer diameter of 26 mm, and a thickness of 3 mm was utilized as the closed thermosyphon system, and also an acrylic tube with a length of 200 mm was used as a heat exchanger at the condenser wall. They tested the closed thermosyphon between the heat flux of 9182 W/m^2 and 21424 W/m^2. The results of this study showed that the decrease of the evaporator temperature is 11% at the heat flux of 9182 W/m^2 and 14% at the heat flux of 21424 W/m^2 as used the self-rewetting fluids instead of water.

Kusuma et al. [18] have studied the thermal performance of a straight vertical closed-thermosyphon that be a passive cooling system on the nuclear-spent fuel pool. For this purpose, the heat pipe was made from a copper tube with a length of 6000 mm (each length of 2000 mm at the evaporator, adiabatic, and condenser), with the outer and inner diameters of 107.6 mm and 106.1 mm, respectively. The water was used as working fluid and charged into the heat pipe with various filling ratios of 40%, 60%, and 80% at different heat loads of 1000 W, 1500 W, 2000 W, and 2500 W. According to the results, the thermal resistance would decrease by increasing the heat load applied to the evaporator and coolant volumetric flow rate when a filling ratio of 80% was charged into the heat pipe. Also, the natural circulation process had occurred more quickly when the heat pipe had the lowest thermal resistance.

According to the previous study in the literature, the experimental studies on the closed thermosyphon have usually performed in the smaller length of that and the equal size of evaporator and condenser regions. Although different fluids have been used as working fluid in the closed thermosyphon, the water has shown better thermal performance in most of the applications. Besides, the closed thermosyphon has steadily been vacuumed and taken into account as constant saturation temperature at a constant vacuum pressure during the experiments in the literature. In this study, the thermal performance of the vacuumed copper pipe was experimentally investigated using different volume values (5 ml, 10 ml, 15 ml, and 20 ml) and inclination angles (45°, 60°, and 90°) for variable vacuum pressures. For this purpose, the inner, outer diameter, and length of the vacuumed pipes filled with the distilled water were 26 mm, 28 mm, and 1500 mm, respectively. This copper pipe was vacuumed until the absolute pressure of 6.32 kPa at one time and immersed in a heat source at a constant temperature of 82°C at the beginning of the experiments. All calculations were performed as variable saturation temperatures at variable vacuum pressures with changing times.

2. Materials and methods

The vacuumed pipes provide efficient heat transfer with phase transition between interfaces due to the evaporating has started in low temperatures at vacuum conditions. The vacuumed pipe was designed as a circular closed tube system, and two-phase flow heat transfer mechanisms were experimentally modeled in cases such as boiling, evaporation, and condensation.

The vacuumed pipe is composed of three different regions; at the bottom is the liquid region, the evaporation region is in the middle, and the condensation region is the other region of that. The valve located at the top of the vacuumed pipe provides the connection between the pipe and the vacuum pump. Also, it controls the filling water liquid inside the vacuumed pipe. The liquid region is the circular closed tube section filled with water liquid from the bottom to a certain height. When the vacuumed pipe is heated, the water liquid in the bottom of the pipe begins to evaporate and runs into the evaporation region. The two-phase flow with increasing temperature will reach the top region of the circular closed tube, and the two-phase fluid will condense because of the lower temperature therein.

2.1. Experimental setup

The thermal performance of vacuumed copper pipe was experimentally investigated using different volume values of 5 ml, 10 ml, 15 ml, and 20 ml with inclination angles of 45°, 60°, and 90° for variable vacuum pressures. For this purpose, the inner, outer diameter, and length of the vacuumed pipes filled with the distilled water were 26 mm, 28 mm, and 1500 mm, respectively. This copper pipe was vacuumed until the absolute pressure of 6.32 kPa at one time and immersed in a heat source at a constant temperature of 82°C at the beginning of the experiments. The surface temperatures of the vacuumed pipes were measured at twenty different points by using K-type thermocouples in two different data loggers. Also, a thermal camera was used to measure the temperature of the vacuumed pipe at different inclination angles. The flow diagram of the designed test apparatus was given in Fig. 1.

According to Fig. 1a, the designed test apparatus consists of computer (A), data loggers (B–C), resistance heater-heat source (D), vacuumed pipe (E), manometer (F), thermocouples (G-Z). The lengths of the twenty different points using K-type thermocouples were shown in Fig. 1b, and the distances of K-type thermocouples were given in Table 1.

This pipe is dipped in the resistance heat source that has the water at the constant temperature of 82°C being over the saturation temperature of 36.78°C at the pressure of 6.32 kPa. Also, the vacuumed copper pipe was filled with the water volume of different values. The experimental period was taken as 10 min for the surface temperature of the vacuumed pipe reaching the constant values. The test apparatus and the ambient of that were given in Fig. 2.

According to Fig. 2, the seven different thermocouples were used to record the average temperature of the evaporation region. In comparison, the eight different thermocouples were used to record the average temperature of the condensation region. Besides, the five different thermocouples were used to record the average temperature of the boiling region.

2.2. Theoretical analysis

The average temperature of the boiling ($T_{boi,ave}$), evaporation ($T_{evap,ave}$), and condensation ($T_{cond,ave}$) for different regions were

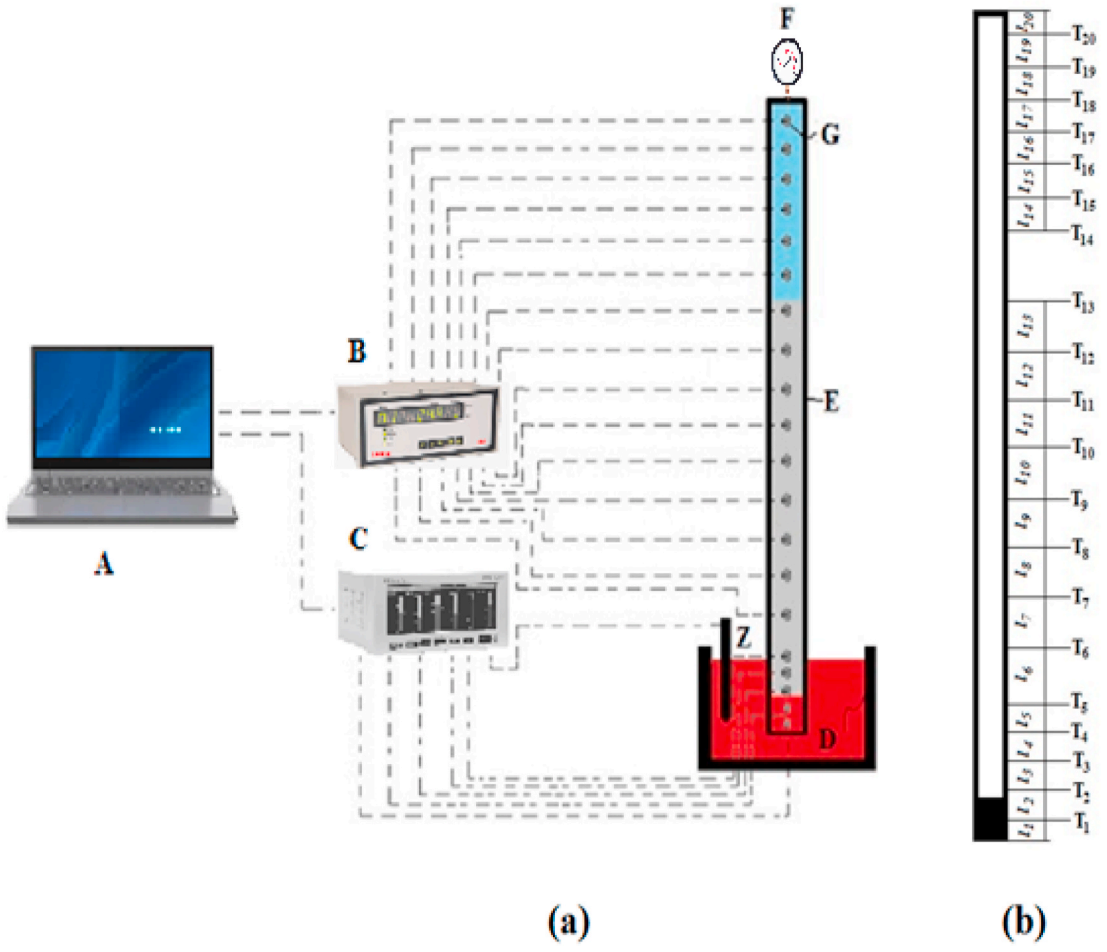

Fig. 1. The flow diagram of the designed test apparatus.

Table 1
The distances of twenty K-type thermocouples.

Lengths	l_1	l_2	l_3	l_4	l_5	l_6	l_7	l_8	l_9	l_{10}
Distance (mm)	10	20	20	20	20	100	100	100	100	100
Lengths	l_{11}	l_{12}	l_{13}	l_{14}	l_{15}	l_{16}	l_{17}	l_{18}	l_{19}	l_{20}
Distance (mm)	100	100	100	50	50	50	50	50	50	20

Fig. 2. The test apparatus and the ambient of that.

monitored experimentally. These average temperatures were calculated as:

$$T_{boi,ave} = \frac{T_1 + T_2 + T_3 + T_4 + T_5}{5} \tag{1a}$$

$$T_{evap,ave} = \frac{T_6 + T_7 + T_8 + T_9 + T_{10} + T_{11} + T_{12} + T_{13}}{8} \tag{1b}$$

$$T_{cond,ave} = \frac{T_{14} + T_{15} + T_{16} + T_{17} + T_{18} + T_{19} + T_{20}}{7} \tag{1c}$$

Grashof number, an essential parameter in natural convection, is defined as an indicator of the ratio of the friction force of the buoyancy effect of a flow element. This dimensionless number is calculated as:

$$Gr_L \equiv \frac{g\beta(T_s - T_\infty)L^3}{\nu^2} \tag{2}$$

here β, ν, T_s, and T_∞ are the volume expansion coefficient, kinematic viscosity, surface, and ambient temperatures. The natural convection correlations for a vertical cylinder in laminar flows can be valid in the surround of the convection of the vacuumed pipe because the boiling region of that is inside the water. In contrast, the condensation region is open to the ambient air. Churchill and Chu [19] proposed a correlation of average Nusselt number for vertical cylinder:

$$\overline{Nu}_L = \left\{0.825 + \frac{0.387Ra_L^{1/6}}{\left[1 + (0.492/Pr)^{9/16}\right]^{8/27}}\right\}^2 \tag{3}$$

Here Ra_L and Pr are Rayleigh and Prandtl numbers, respectively [20]. Although Eq. (3) is valid for all Rayleigh numbers, this equation is only used for the circumstance of $D/L \gtrsim 35/Gr_L^{1/4}$. The different correlations used for thin long vertical cylinders are necessary because Eq. (3) did not meet this circumstance in this study. For this reason, the Nusselt number for the pipe with the length of H and diameter of D is given [21,22]:

$$\overline{Nu}_H = \frac{4}{3}\left[\frac{7Ra_H Pr}{5(20 + 21Pr)}\right]^{1/4} + \frac{4(272 + 315Pr)H}{35(64 + 63Pr)D} \tag{4}$$

$$Ra_H = \frac{g\beta\Delta T H^3}{\alpha\nu} \tag{5}$$

here $\Delta T$is the temperature difference between the pipe surface and the fluid reservoir while α denotes the thermal diffusivity. Although Eq. (4) is valid for all Rayleigh numbers, this equation is only used for the circumstance of $D/H > Ra_H^{-1/4}$. The wall-averaged heat transfer coefficient and the total heat transfer rate are calculated as:

$$\overline{h} = \frac{k.\overline{Nu}_H}{H} \tag{6}$$

$$\dot{Q} = \overline{h}(\pi \times D \times L_b)\Delta T \tag{7}$$

The mean heat transfer coefficient (h_{boi}) of the boiling region were calculated as [23,24]:

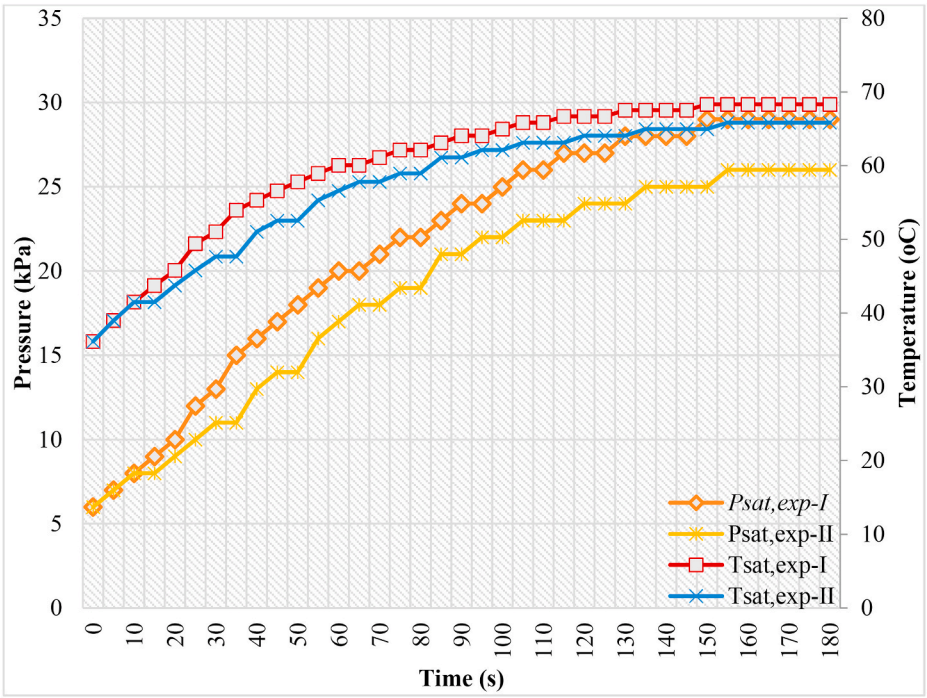

Fig. 3. The change of the saturation temperature and pressure inside the vacuumed copper pipe for different time steps.

$$h_{boi} = \frac{\dot{Q}}{(\pi \times D \times L_b)(T_{boi,ave} - T_{sat})} \tag{8}$$

here T_{sat} is the saturation temperature. Besides, the mean heat transfer coefficient (h_{cond}) of the condensation region of the vacuum pipe is calculated with the help of the equation given below [20]:

$$h_{cond} = \frac{\overline{Nu}_{cond}.k_s}{L_c} = 0.943\left[\frac{g.\rho_l(\rho_l - \rho_v)k_l^3.h'_{fg}}{\mu_l(T_{sat} - T_{cond,ave})L_c}\right]^{1/4} \tag{9}$$

here $\overline{Nu}_{cond}$ and h'_{fg} denote the mean average Nusselt number and corrected latent heat of vaporization obtained by considering the mass transportation caused by thermal effects, respectively. Also, h'_{fg} is calculated as:

$$h'_{fg} = h_{fg}(1 + 0.68\,Ja) \tag{10}$$

here Ja is Jakob number and it is calculated as:

$$Ja = c_{p,l}\,(T_{sat} - T_{cond,ave}) \tag{11}$$

Besides thermal resistance (R) of the vacuumed pipe is defined [24]:

$$R = \frac{(T_{boi,ave} - T_{cond,ave})}{\dot{Q}} \tag{12}$$

For the evaporation-condensation mechanism, the average saturation temperature was defined by using the vacuum pressure given in Fig. 3 because the pressure has changed with increasing temperature at different times. On the other hand, the values of water

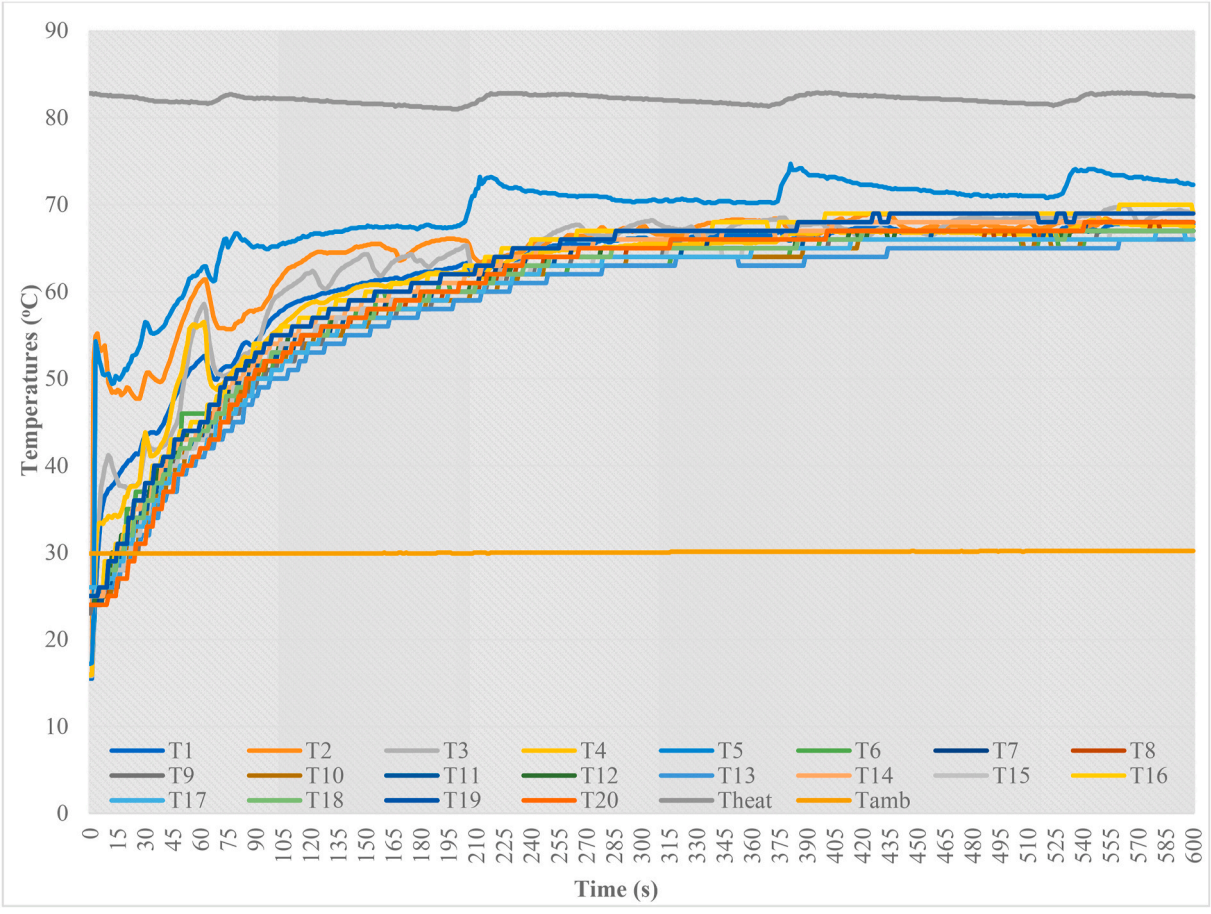

Fig. 4. The change of temperatures at all thermocouples in the vacuumed copper pipe with the water volume of 10 ml at the inclination angle of 90°.

density (ρ_{water}) and surface tension (σ_{w-s}) between phases for two multiphase are calculated by using the following equations [25]:

$$\rho_{water} = 750.4359 + 2.14358 \times T - 0.0051 \times T^2 + 2.27243e^{-06} \times T^3 \quad (13)$$

$$\sigma_{w-s} = 0.083112 + 0.000107 \times T - 5.8e^{-07} \times T^2 + 3.15661e^{-10} \times T^3 \quad (14)$$

ρ_{water} and σ_{w-s} values have been calculated for different temperature values inside the vacuumed copper pipe.

The measurements were evaluated with the uncertainty analysis. The average of the measured values is given by ($\overline{X}$):

$$\overline{X} = \frac{\sum X_m}{n} \quad (15)$$

where n; the numbers of the measurement and X_m; the measured value. Standard deviation (SD) is given as follows:

$$SD = \sqrt{\frac{\sum_{m=1}^{n}\left(X_m - \overline{X}\right)^2}{(n-1)}} \quad (16)$$

Then, uncertainty (U) is given by Eq. (15) as following [26]:

$$U = \frac{SD}{\sqrt{n}} \quad (17)$$

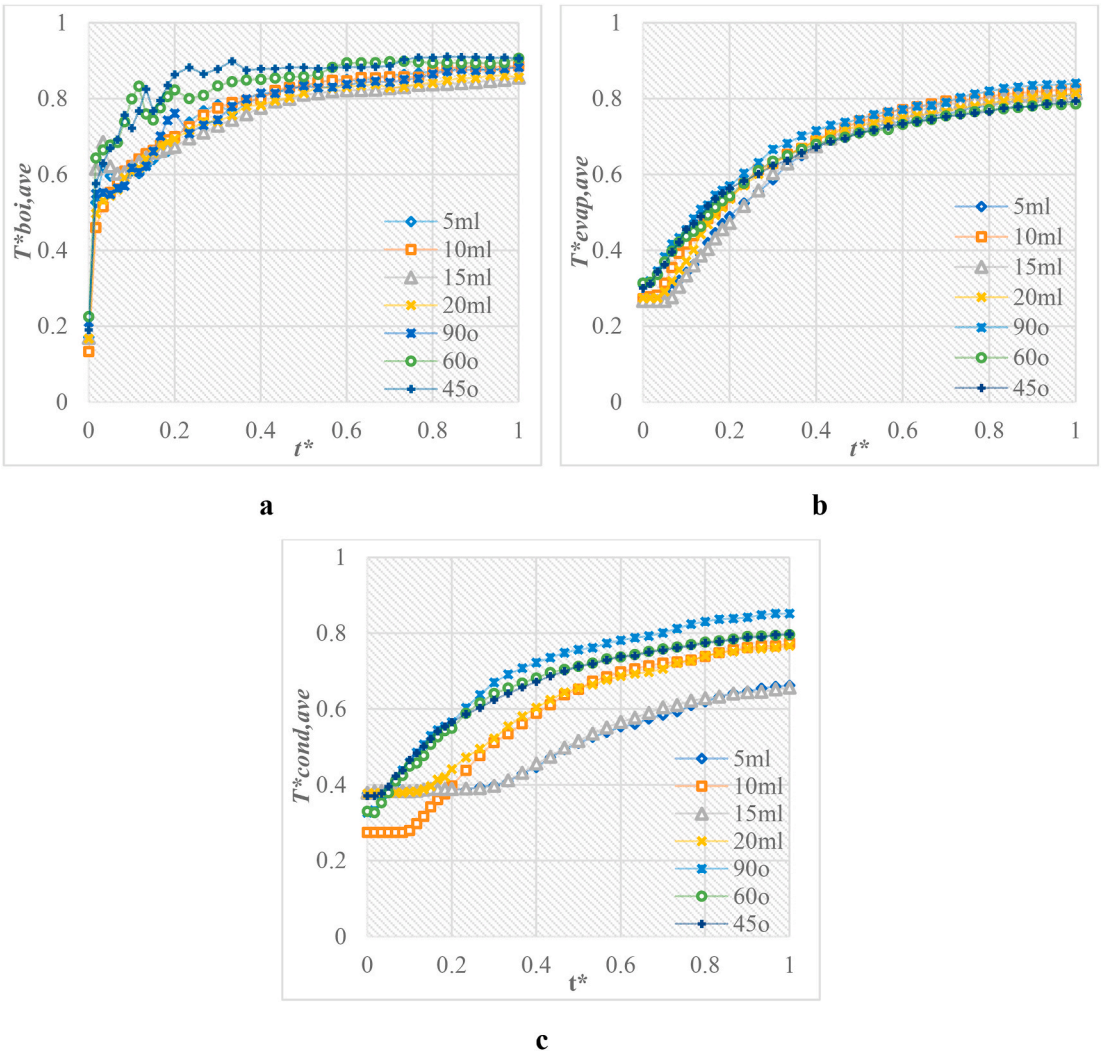

Fig. 5. *The change dimensionless (a) $T^*_{boi,ave}$, (b) $T^*_{evap,ave}$, and (c) $T^*_{cond,ave}$ in the vacuumed copper pipe with all water volumes and inclination angles.*

3. Results and discussion

A comprehensive experimental study was performed for the thermal performance analysis of the closed thermosyphon in detail. The material of the closed thermosyphon was chosen as copper; the inner, outer diameter, and length of the vacuumed pipe that was filled with the distilled water were selected as 26 mm, 28 mm, and 1500 mm, respectively. Also, this thermosyphon was vacuumed until the absolute pressure of 6.32 kPa and immersed in a heat source at a constant temperature of 82°C at the beginning of the experiments. The change of temperatures at all thermocouples in the vacuumed copper pipe with the water volume of 10 ml at the inclination angle of 90° is given in Fig. 4.

According to Fig. 4, it is seen that the upper part of the thermosyphon gets warmer over time with the fluctuations. At first, the highest temperature was reached at T5, and then this value started to increase again after a certain period of decrease. This point is where the heat load was supplied to the thermosyphon, and there was low-density air depending on the vacuum inside the thermosyphon. On the other hand, there was no significant change in the heater and ambient temperatures during the experiment period. Besides these, the temperature values have become the steady-state condition after 300 s because the temperature values for all thermocouples have changed below the value of 0.5°C after this time. The change of dimensionless (a) $T^*_{boi,ave}$, (b) $T^*_{evap,ave}$, and (c) $T^*_{cond,ave}$ in the vacuumed copper pipe with all water volumes and inclination angles is given in Fig. 5.

According to Fig. 5a, the temperature of the vacuumed copper pipe first increased rapidly in the first dimensionless time of 0.2, then decreased slightly, and then started to increase again for vacuum copper pipes with different initial temperatures.

Besides, in Fig. 5b, while $T^*_{evap,ave}$ value of the vacuumed copper pipe with the same initial temperatures increased continuously

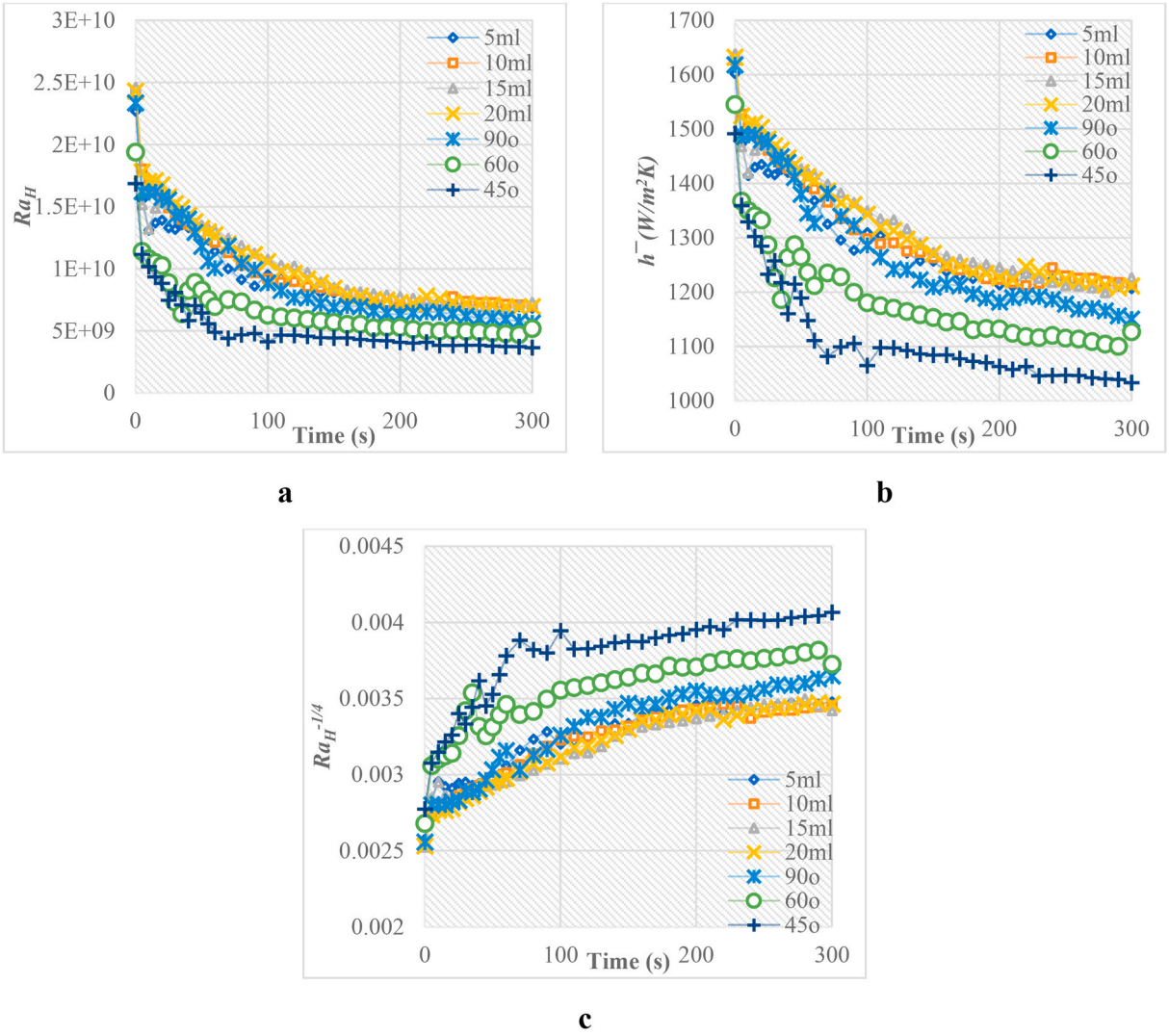

Fig. 6. *The change of Ra_H, $\overline{h}$, and $Ra_H^{-1/4}$ values for the boiling region in the vacuumed copper pipe with all water volumes and inclination angles.*

until the end of the experiment, a faster increase was observed in 10 ml and 20 ml liquid volumes while $T^*_{evap,ave}$ values have increased continuously at the inclination angles of 90°, 60°, and 45° during the experiment. From this point on, $T^*_{evap,ave}$ value of the 5 ml liquid volume has tended to drop slightly while it has remained essentially constant at other liquid volume values. On the other hand in Fig. 5c, $T^*_{cond,ave}$ of the vacuumed copper pipe containing 10 ml liquid volume at a dimensionless initial temperature of 0.27 and containing 45°, 15 ml, and 20 ml liquid volumes at dimensionless initial temperatures of about 0.37 shows a steady increase until the end of the experiment. Also, $T^*_{cond,ave}$ values for all inclination angles and water volumes have shown a similar trend with slight differences in increase-decrease values. The change of Ra_H, $\overline{h}$, and $Ra_H^{-1/4}$ values for the boiling region in the vacuumed copper pipe with all water volumes and inclination angles are given in Fig. 6.

According to Fig. 6a, Ra_H values have shown a similar trend for the vacuumed copper pipe with all water volumes and inclination angles. Besides, Ra_H values at the inclination angles of 45° and 60° were lower than the others for all seconds. Ra_H values have changed between $3.65x10^9$ and $2.46x10^{10}$ for the vacuumed copper pipe with all water volumes and inclination angles. Besides these in Fig. 6b, $\overline{h}$ values have decreased with increasing time for the vacuumed copper pipe with all water volumes and inclination angles. The maximum $\overline{h}$ value was calculated as 1226.69 W/m^{2}K in the vacuumed copper pipe with the water volume of 15 ml at the inclination angle of 90° while the minimum $\overline{h}$ value was found as 1033.72 W/m^{2}K in the vacuumed copper pipe with the water volume of 10 ml at the inclination angle of 45° for the time of 300th second. According to Fig. 6c, $Ra_H^{-1/4}$ values for the vacuumed copper pipe with all water volumes and inclination angles were below the D/H value (0.28) of this study. Therefore, the calculated $\overline{h}$ values have been valid for the usage of this work. The change of h_{boi} and h_{cond} values in the vacuumed copper pipe with all water volumes and inclination angles are given in Fig. 7.

According to Fig. 7a, h_{boi} values have generally decreased with increasing time for the vacuumed copper pipe with all water volumes and inclination angles while decreasing and increasing fluctuations. After 240 s, h_{boi} values have reached the steady-state because of the difference among h_{boi} values stayed a little at that time. On the other hand in Fig. 7b, h_{cond} values in the vacuumed copper pipe with the water volume of 5 ml–15 ml and the inclination angles of 45°-60° showed the horizontal trend with increasing time. The other h_{cond} values have permanently increased after 240th second with increasing time. h_{boi} and h_{cond} values were assessed after the time of 150th second because $T_{boi,ave}$ values stayed below T_{sat} values for the times before that. For this reason, h_{boi} were calculated as negative values before the time of 150th second. h_{boi} and h_{cond} values have been assessed after 240th seconds because the evaporation and condensation have been steady from this time. Also, it was clear that the temperature difference was below 0.5°C after 300th seconds.

The calculated heat transfer coefficients should be compared to the literature values to ensure the validity of the results of this study. For this purpose, the experimental heat transfer coefficients were compared with the correlations of Shiraishi et al. [27] and Imura et al. [28] from the literature [29].

$$h_{boi,Shi} = 0.32\left(\frac{\rho_{water}^{0.65} k_{water}^{0.3} c_{p\,water}^{0.7} g^{0.2}}{\rho_{vapor}^{0.25} h_{fg}^{0.4} \mu_{water}^{0.1}}\right)\left(\frac{P_{vapor}}{P_{atm}}\right)^{0.23}\left(\frac{\dot{Q}}{A_{boi}}\right)^{0.4} \tag{18}$$

$$h_{boi,Imu} = 0.32\left(\frac{\rho_{water}^{0.65} k_{water}^{0.3} c_{p\,water}^{0.7} g^{0.2}}{\rho_{vapor}^{0.25} h_{fg}^{0.4} \mu_{water}^{0.1}}\right)\left(\frac{P_{vapor}}{P_{atm}}\right)^{0.3}\left(\frac{\dot{Q}}{A_{boi}}\right)^{0.4} \tag{19}$$

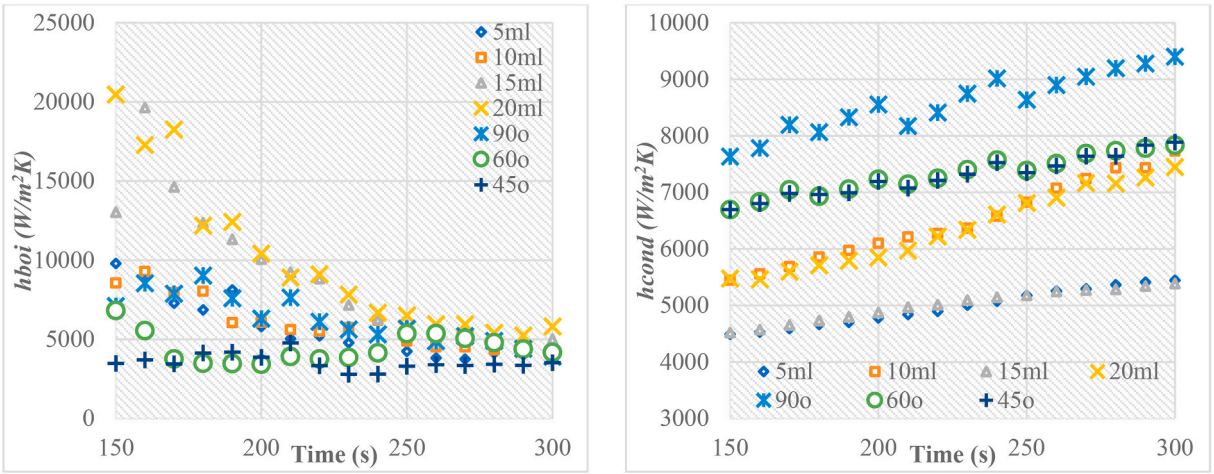

Fig. 7. *The change of h_{boi} and h_{cond} values in the vacuumed copper pipe with all water volumes and inclination angles.*

here k_{water}, $c_{p_{water}}$, and μ_{water} were thermal conductivity, isobaric specific heat, and viscosity of water while P_{vapor} and ρ_{vapor} were the pressure and density of vapor, respectively. Also, g was the gravitational acceleration, and the change this value was considered of the inclination angles.

$h_{boi,Shi}$ versus h_{boi} values in the vacuumed copper pipe with the water volume of 5 ml, 10 ml, 15 ml, and 20 ml at the inclination angle of 90° were in the range of -20% and 20%, although some values surpassed this range a little. Besides, $h_{boi,Shi}$ versus h_{boi} values in the vacuumed copper pipe with the water volume of 10 ml at the inclination angle of 45°, 60°, and 90° were in the range of -20% and 20% despite some values have surpassed these ranges a little. The change of mean error among $h_{boi,Imu}$ versus h_{boi} values in the vacuumed copper pipe with all water volumes and inclination angles were given in Table 2.

According to Table 2, the mean absolute error among $h_{boi,Shi}$ versus h_{boi} values were calculated as 19.69%, 13.09%, 10.50%, and 17.36% for the water volume of 5 ml, 10 ml, 15 ml, and 20 ml, respectively, while these values were calculated as 19.14%, 13.36%, and 11.69% for the inclination angle of 45°, 60°, and 90°, respectively. On the other hand, the mean error among $h_{boi,Imu}$ versus h_{boi} values were calculated as 10.83% for the inclination angle of 45°, and this value was better than the mean error of $h_{boi,Shi}$ of that. Beside this, the mean error among $h_{boi,Imu}$ versus h_{boi} values were found as 11.43% and 8.53% for the water volume 5 ml and 10 ml, respectively, and also these values were lower than the mean errors of $h_{boi,Shi}$ of that. On the other hand, the other mean error among $h_{boi,Imu}$ versus h_{boi} values were worse than the mean errors of $h_{boi,Shi}$ of that.

The experimental boiling heat transfer coefficients showed a good agreement with the correlations of Shiraishi et al. [27] and Imura et al. [28]. This study's mean error values have shown a similar trend with the study containing the mean error between 2.6% and 36% [30] for water as the working fluid in the literature. Also, these values in this study have been better than the study containing the mean error of 14.3% [31] and the mean error between 14.99% and 24.28% [29] for some cases. These correlations have usually been used for the nucleate boiling conditions in the closed thermosyphons, and these conditions have been valid for the temperature difference being nearly between 4°C and 30°C [32]. After 300th second, Shiraishi et al. and Imura et al. correlations have not demonstrated good results with the experimental results in this study because the temperature difference among the boiling and saturation temperatures have decreased the values of 2–3°C. The change of R values for all water volumes and inclination angles at all times was given in Fig. 8.

According to Fig. 8, R values for all water volumes and inclination angles have shown increasing and decreasing fluctuations. The minimum R values were obtained in the vacuumed copper pipe with a water volume of 10 ml at the inclination angle of 90° until the end of the experiment. On the other hand, the maximum R values were calculated in the vacuumed copper pipe with the water volume of 5 ml at the inclination angle of 90° after 120th second. R values were calculated as 0.0774, 0.0659, and 0.0404 for the inclination angles of 45°, 60°, and 90°, respectively, while these values were obtained as 0.1009, 0.0454, 0.0899, and 0.0403 for the water volumes of 5 ml, 10 ml, 15 ml, and 20 ml, respectively at the time of 300th second.

The measurement devices' technical properties and the uncertainty values of the measurement equipment for different water volumes and inclination angles were given in Table 3 and Table 4, respectively.

According to Table 4, the maximum uncertainty value was obtained as ±0.63 °C at T13 in the experiment of the vacuumed copper pipe with a water volume of 5 ml at the inclination angle of 90°. In comparison, the minimum error was calculated as ±0.06°C at T5 in the experiment of the vacuumed copper pipe with a water volume of 10 ml at the inclination angle of 45°. On the other hand, the uncertainty values were calculated as ±1.20 kPa and ±1.08 kPa for the experiment I and II.

4. Conclusion

In this study, the thermal performance of the vacuumed copper pipe was experimentally investigated using different volume values (5 ml, 10 ml, 15 ml, and 20 ml) and inclination angles (45°, 60°, and 90°) for variable vacuum pressures. For this purpose, the inner, outer diameter, and length of the vacuumed pipes filled with the distilled water were 26 mm, 28 mm, and 1500 mm, respectively. This copper pipe was vacuumed until the absolute pressure of 6.32 kPa at one time and immersed in a heat source at a constant temperature of 82°C at the beginning of the experiments. All calculations were performed as variable saturation temperatures at variable vacuum pressures with changing the time.

The main results of this experimental study are given as:

1 $\overline{h}$ values have decreased with increasing time for the vacuumed copper pipe with all water volumes and inclination angles. $Ra_H^{-1/4}$ values for the vacuumed copper pipe with all water volumes and inclination angles were below the D/H value (0.28) of this study. Therefore, the calculated $\overline{h}$ values have been valid for the usage of this work.
2 h_{boi} and h_{cond} values have been assessed after 240th seconds because the evaporation and condensation have been steady from this time. Also, it was clear that the temperature difference was below 0,5°C after 300th seconds.
3. The absolute minimum errors among $h_{boi,Shi}$ versus h_{boi} values were calculated as 10.50% and 17.36% for the water volume of 15 ml, and 20 ml, respectively, while these values were calculated as 13.36%, and 11.69% for the inclination angle of 60° and 90°, respectively. On the other hand, the minimum errors among $h_{boi,Imu}$ versus h_{boi} values were calculated as 10.83% for the inclination angle of 45°, while these values were found as 11.43% and 8.53% for the water volume 5 ml and 10 ml, respectively.
4. The minimum R values were obtained in the vacuumed copper pipe with a water volume of 10 ml at the inclination angle of 90° until the end of the experiment. On the other hand, the maximum R values were calculated in the vacuumed copper pipe with the water volume of 5 ml at the inclination angle of 90° after 120th second.

Table 2
The change of mean error among $h_{boi,Shi}$ and $h_{boi,Imu}$ versus h_{boi} values in the vacuumed copper pipe with all water volumes and inclination angles.

Parameters	5 ml	10 ml	15 ml	20 ml	45°	60°	90°
Mean Error of $h_{boi,Shi}$ (%)	19.69	13.09	10.50	17.36	19.14	13.36	11.69
Mean Error of $h_{boi,Imu}$ (%)	11.43	8.53	20.96	29.43	10.83	21.91	20.23

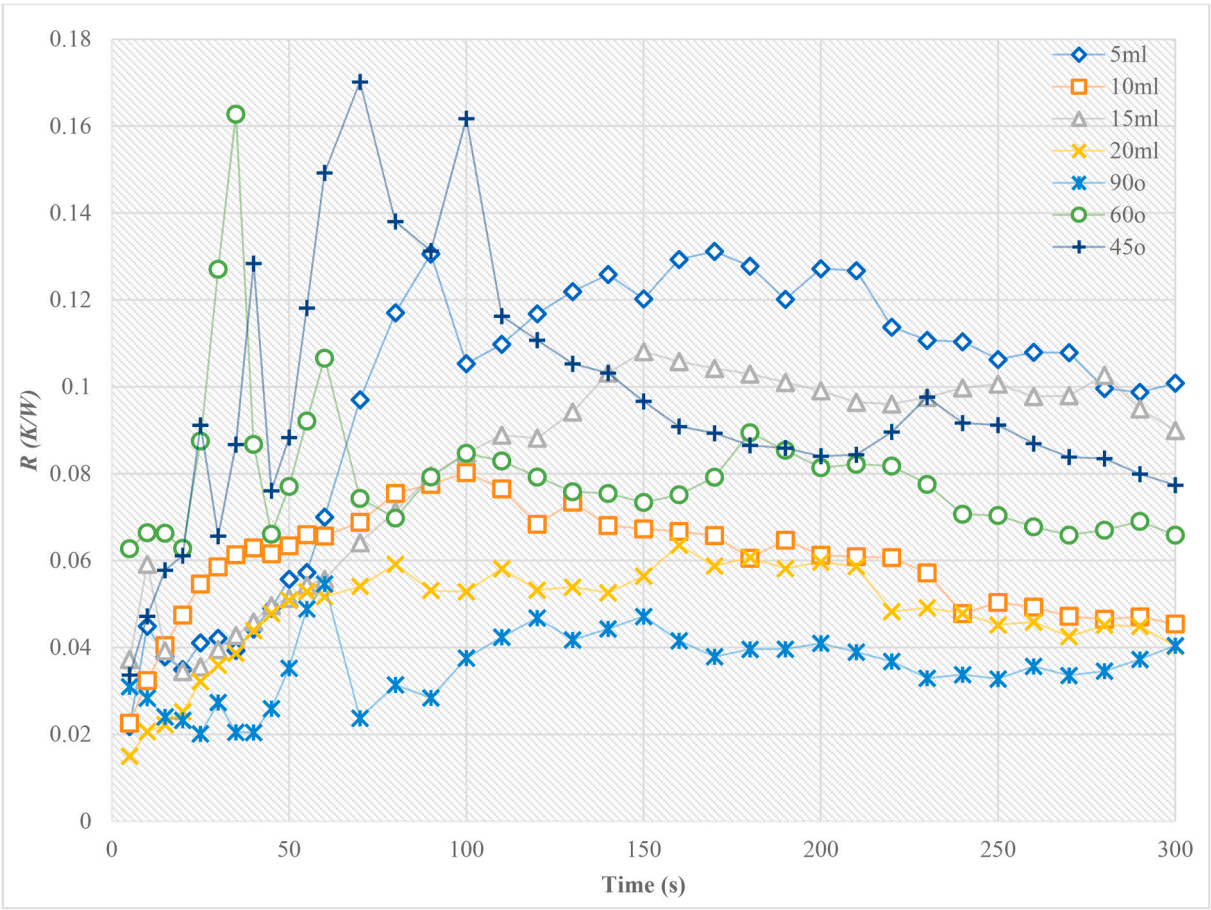

Fig. 8. *The change of R values for all water volumes and inclination angles for all times.*

Table 3
Technical properties of the measurement devices.

Measurement Devices	Technical Properties	Accuracy
Thermocouples (T1-T20)	K-type thermocouple.	±1.5 °C or ±1.5% of measurement value (Whichever is greater)
Vacuum Manometer	Pakkens, Analog Ø100 Manometer.	± 1% over full scale.
Data Logger-1	Elimko PR-100, 12 channels.	±0.5% of recording value or ± 1 °C.
Data Logger-2	Elimko E-680 32 channels.	±0.5% of recording value.

5 The maximum *U* value was obtained as ±0.63°C at T13 in the experiment of the vacuumed copper pipe with the water volume of 5 ml at the inclination angle of 90°. In comparison, the minimum of that was calculated as ±0.06°C at T5 in the experiment of the vacuumed copper pipe with the water volume of 10 ml at the inclination angle of 45°. On the other hand, *U* values were calculated as ±1.20 kPa and ±1.08 kPa for the experiment I and II, respectively.

The experimental boiling heat transfer coefficients showed a good agreement with the correlations of Shiraishi et al. [27] and Imura et al. [28]. This study's mean error values have shown a similar trend with the study containing the mean error between 2.6% and 36%

Table 4
The uncertainty values of the measurement equipment for different water volumes and inclination angles.

Thermocouples	*U* (°C)						
	90°	60°	45°	5 ml	10 ml	15 ml	20 ml
T1	0.30	0.12	0.09	0.27	0.27	0.24	0.24
T2	0.21	0.19	0.13	0.23	0.25	0.17	0.22
T3	0.32	0.18	0.10	0.26	0.30	0.24	0.28
T4	0.31	0.28	0.15	0.22	0.29	0.25	0.27
T5	0.21	0.13	0.06	0.18	0.25	0.17	0.22
T6	0.36	0.38	0.31	0.39	0.42	0.40	0.39
T7	0.42	0.37	0.33	0.40	0.40	0.39	0.36
T8	0.40	0.36	0.32	0.37	0.40	0.37	0.43
T9	0.43	0.38	0.36	0.37	0.40	0.44	0.42
T10	0.39	0.38	0.32	0.43	0.43	0.38	0.40
T11	0.39	0.36	0.31	0.43	0.40	0.41	0.39
T12	0.38	0.35	0.33	0.48	0.44	0.47	0.43
T13	0.43	0.37	0.37	0.63	0.48	0.62	0.47
T14	0.42	0.36	0.32	0.59	0.50	0.59	0.50
T15	0.40	0.39	0.34	0.55	0.49	0.50	0.53
T16	0.41	0.38	0.34	0.51	0.52	0.51	0.51
T17	0.43	0.39	0.33	0.45	0.53	0.45	0.52
T18	0.39	0.37	0.33	0.41	0.50	0.40	0.49
T19	0.40	0.37	0.34	0.37	0.42	0.33	0.45
T20	0.44	0.37	0.34	0.32	0.34	0.30	0.44

[30] for water as the working fluid in the literature. Also, these values in this study have been better than the study containing the mean error of 14.3% [31] and the mean error between 14.99% and 24.28% [29] for some cases. These correlations have usually been used for the nucleate boiling conditions in the closed thermosyphons, and these conditions have been valid for the temperature difference being nearly between 4°C and 30°C [32]. After 300th second, Shiraishi et al. and Imura et al. correlations have not demonstrated good results with the experimental results in this study because the temperature difference among the boiling and saturation temperatures have decreased the values of 2–3°C. Furthermore, the comprehensive numerical analysis development will continue as a parametric study in detail by using this experimental study.

Author statement

Dr. Halit Arat: Conducting a research and investigation process, specifically performing the experiments, or data/evidence collection (Investigation), Conceptualization, Methodology, Validation, Investigation, Resources, Data Curation, Writing - Original Draft, Writing - Review & Editing, Visualization. Prof. Dr. Oguz Arslan: Conceptualization, Methodology, Writing - Original Draft, Writing - Review & Editing, Visualization, Supervision. Ass. Prof. Dr. Umran Ercetin: Conducting a research and investigation process, specifically performing the experiments, or data/evidence collection (Investigation), Application of statistical, mathematical, computational, or other formal techniques to analyze or synthesize study data (Formal Analysis). Assoc. Prof. Dr. Abdullah Akbulut: Conceptualization, Methodology, Writing - Review & Editing, Visualization, Supervision.

Declaration of competing interest

The authors declare that they have no known competing financial interests or personal relationships that could have appeared to influence the work reported in this paper.

Acknowledgment

This study was supported by Kutahya Dumlupinar University Scientific Research Projects Unit (DPU-BAP) under the grant of the project number of 2017-55.

Halit Arat, 1st author, would like to thank Technological Research Council of Turkey, National Scholarship Program for Ph.D. students (TUBITAK-BIDEB) for its financial assistance during his doctoral studies.

References

[1] H. Arat, O. Arslan, Exergoeconomic analysis of district heating system boosted by the geothermal heat pump, Energy 119 (2017) 1159–1170, https://doi.org/10.1016/j.energy.2016.11.073.

[2] B.C. Nookaraju, P.S.V. Kurma Rao, S. Nagasarada, Experimental and numerical analysis of thermal performance in heat pipes, in: Procedia Eng., Elsevier Ltd, 2015, pp. 800–808, https://doi.org/10.1016/j.proeng.2015.11.415.

[3] N.K. Gupta, A.K. Tiwari, S.K. Ghosh, Heat transfer mechanisms in heat pipes using nanofluids – a review, Exp. Therm. Fluid Sci. 90 (2018), https://doi.org/10.1016/j.expthermflusci.2017.08.013.

[4] D. Schneider, M. Lauer, I. Voigt, W.G. Drossel, Development and examination of switchable heat pipes, Appl. Therm. Eng. 99 (2016) 857–865, https://doi.org/10.1016/j.applthermaleng.2016.01.086.
[5] Jong Hoon Jang, A. Faghri, Won Soon Chang, Analysis of the one-dimensional transient compressible vapor flow in heat pipes, Int. J. Heat Mass Tran. 34 (1991), https://doi.org/10.1016/0017-9310(91)90214-Y.
[6] Y. Gao, Y. Cui, B. Xu, B. Sun, X. Zhao, H. Li, L. Chen, Two phase flow heat transfer analysis at different flow patterns in the wellbore, Appl. Therm. Eng. 117 (2017) 544–552, https://doi.org/10.1016/j.applthermaleng.2017.02.058.
[7] A.W. Badar, R. Buchholz, F. Ziegler, Single and two-phase flow modeling and analysis of a coaxial vacuum tube solar collector, Sol. Energy 86 (2012) 175–189, https://doi.org/10.1016/j.solener.2011.09.021.
[8] J. Venkata Suresh, P. Bhramara, CFD analysis of multi turn pulsating heat pipe, in: Mater. Today Proc., Elsevier Ltd, 2017, pp. 2701–2710, https://doi.org/10.1016/j.matpr.2017.02.146.
[9] D. Zhang, H. Tao, M. Wang, Z. Sun, C. Jiang, Numerical simulation investigation on thermal performance of heat pipe flat-plate solar collector, Appl. Therm. Eng. 118 (2017) 113–126, https://doi.org/10.1016/j.applthermaleng.2017.02.089.
[10] W. Rivera, A. Xicale, Heat transfer coefficients in two phase flow for the water/lithium bromide mixture used in solar absorption refrigeration systems, Sol. Energy Mater. Sol. Cells 70 (2001) 309–320, https://doi.org/10.1016/S0927-0248(01)00073-3.
[11] S. Korniliou, C. Mackenzie-Dover, J.R.E. Christy, S. Harmand, A.J. Walton, K. Sefiane, Two-dimensional heat transfer coefficients with simultaneous flow visualisations during two-phase flow boiling in a PDMS microchannel, Appl. Therm. Eng. 130 (2018), https://doi.org/10.1016/j.applthermaleng.2017.11.003.
[12] J.V. Suresh, P. Bhramara, CFD analysis of copper closed loop pulsating heat pipe, in: Mater. Today Proc., Elsevier Ltd, 2018, pp. 5487–5495, https://doi.org/10.1016/j.matpr.2017.12.138.
[13] H. Jouhara, Z. Ajji, Y. Koudsi, H. Ezzuddin, N. Mousa, Experimental investigation of an inclined-condenser wickless heat pipe charged with water and an ethanol-water azeotropic mixture, Energy 61 (2013), https://doi.org/10.1016/j.energy.2012.09.033.
[14] M.M. Sarafraz, F. Hormozi, S.M. Peyghambarzadeh, Thermal performance and efficiency of a thermosyphon heat pipe working with a biologically ecofriendly nanofluid, Int. Commun. Heat Mass Tran. 57 (2014), https://doi.org/10.1016/j.icheatmasstransfer.2014.08.020.
[15] E. Gedik, Experimental investigation of the thermal performance of a two-phase closed thermosyphon at different operating conditions, Energy Build. 127 (2016), https://doi.org/10.1016/j.enbuild.2016.06.066.
[16] J. Seo, J.Y. Lee, Length effect on entrainment limitation of vertical wickless heat pipe, Int. J. Heat Mass Tran. 101 (2016), https://doi.org/10.1016/j.ijheatmasstransfer.2016.05.096.
[17] Y. Naresh, K. Shri Vignesh, C. Balaji, Experimental investigations of the thermal performance of self-rewetting fluids in internally finned wickless heat pipes, Exp. Therm. Fluid Sci. 92 (2018), https://doi.org/10.1016/j.expthermflusci.2017.10.037.
[18] M.H. Kusuma, N. Putra, A.R. Antariksawan, R.A. Koestoer, S. Widodo, S. Ismarwanti, B.T. Verlambang, Passive cooling system in a nuclear spent fuel pool using a vertical straight wickless-heat pipe, Int. J. Therm. Sci. 126 (2018), https://doi.org/10.1016/j.ijthermalsci.2017.12.033.
[19] S.W. Churchill, H.H.S. Chu, Correlating equations for laminar and turbulent free convection from a vertical plate, Int. J. Heat Mass Tran. 18 (1975), https://doi.org/10.1016/0017-9310(75)90243-4.
[20] T.L. Bergman, A.S. Lavine, F.P. Incropera, D.P. DeWitt, Principles of Heat and Mass Transfer, Palme Pub., 2015.
[21] A.J. Le Fevre, E.J. Ede, Laminar free convection from the outer surface of a vertical circular cylinder, Proc. 9th Int. Congr. Appl. Mech. 4 (1956) 175–183.
[22] A. Bejan, Convection Heat Transfer, fourth ed., 2013, https://doi.org/10.1002/9781118671627.
[23] A. Ozsoy, V. Corumlu, Thermal performance of a thermosyphon heat pipe evacuated tube solar collector using silver-water nanofluid for commercial applications, Renew. Energy 122 (2018) 26–34, https://doi.org/10.1016/j.renene.2018.01.031.
[24] Z.H. Liu, Y.Y. Li, R. Bao, Compositive effect of nanoparticle parameter on thermal performance of cylindrical micro-grooved heat pipe using nanofluids, Int. J. Therm. Sci. 50 (2011) 558–568, https://doi.org/10.1016/j.ijthermalsci.2010.11.013.
[25] NIST Reference Database, REFPROP 9 (2010), .0.
[26] M. Senturk Acar, O. Arslan, Performance analysis of a new hybrid cooling–drying system, Environ. Prog. Sustain. Energy 37 (2018) 1808–1828, https://doi.org/10.1002/ep.12832.
[27] M. Shiraishi, K. Kikuchi, T. Yamanishi, Investigation of heat transfer characteristics of a two-phase closed thermosyphon, J. Heat Recovery Syst. 1 (1981), https://doi.org/10.1016/0198-7593(81)90039-4.
[28] H. Imura, K. Sasaguchi, H. Kozai, S. Numata, Critical heat flux in a closed two-phase thermosyphon, Int. J. Heat Mass Tran. 26 (1983), https://doi.org/10.1016/s0017-9310(83)80172-0.
[29] R. Andrzejczyk, Experimental investigation of the thermal performance of a wickless heat pipe operating with different fluids: water, ethanol, and SES36. Analysis of influences of instability processes at working operation parameters, Energies 12 (2019), https://doi.org/10.3390/en12010080.
[30] F. Táboas, M. Vallès, M. Bourouis, A. Coronas, Pool boiling of ammonia/water and its pure components: comparison of experimental data in the literature with the predictions of standard correlations, Int. J. Refrig. 30 (2007), https://doi.org/10.1016/j.ijrefrig.2006.12.009.
[31] M.M. Mahmoud, T.G. Karayiannis, Heat transfer correlation for flow boiling in small to micro tubes, Int. J. Heat Mass Tran. 66 (2013), https://doi.org/10.1016/j.ijheatmasstransfer.2013.07.042.
[32] V. Guichet, S. Almahmoud, H. Jouhara, Nucleate pool boiling heat transfer in wickless heat pipes (two-phase closed thermosyphons): a critical review of correlations, Therm. Sci. Eng. Prog. 13 (2019), https://doi.org/10.1016/j.tsep.2019.100384.